

Friction Stir Welding for Marine Applications: Mechanical Behaviour and Microstructural Characteristics of Al-Mg-Si-Cu Plates

Liane Roldo^a, Nenad Vulić^b

Friction stir welding is a multipurpose solid-state joining process mainly used for aluminium and steel plates and frames. Friction stir welded non-ferrous metallic alloys, similar or dissimilar, in particular aluminium alloys, provide opportunities for the improvement and development of new product designs. This paper investigates the correlation between the mechanical behaviour and morphological structures of friction stir welded Al-Mg-Si(Cu) alloy plates in two temper conditions. Micro Vickers hardness and tensile tests were carried out. Additionally, morphology was investigated using optical microscopy and scanning electron microscopy. Samples subjected to the post weld heat treatment were shown to have the best properties owing to the formation of a significant number of hardening particles which, added to the nugget grain refinement, resulted in the increase of the material strength.

KEY WORDS

- ~ Friction stir welding
- ~ Al-Mg-Si-Cu alloy
- ~ Shipbuilding
- ~ Solid-state welding


a. Federal University of Rio Grande do Sul, Materials Department, Brazil

e-mail: liane.roldo@gmail.com

b. University of Split, Faculty of Maritime Studies, Split, Croatia

e-mail: nenad.vulic@pfst.hr

doi: 10.7225/toms.v08.n01.008

This work is licensed under 

1. INTRODUCTION

After two decades of research and collection of data on friction stir welding (FSW), the technological progress achieved in the area can be logically and fairly said to prove the reliability of the FSW, especially when it comes to aluminium alloys.

As a solid-state welding process, FSW causes less distortion and changes in metallurgical and mechanical properties compared to conventional fusion processes (Mishra and Ma, 2005; Mishra, Partha and Kumar, 2014). The transversal tool movement produces an intricate material flow pattern, which varies depending on the following parameters: tool geometry and workpiece penetration, heat flow, tilt angle, rotational and transverse speed (Chao et al., 2003; Galvão et al., 2010; Leal et al., 2008; Sun et al., 2013; Velichko et al., 2016).

Post-welding aging treatments tend to increase microhardness in the weld zone. However, in some circumstances they may also increase or decrease elongation, yield and tensile strength, as well as the fatigue crack propagation rate (Cerri and Leo, 2013; Malopheyev, S. et al., 2016; Mishra, Partha and Kumar, 2014).

The research on the FSW process and its weldable alloys focuses on a wide range of structures. Typical uses are from window frames to heavily loaded structures, like airframes, aerospace parts, oil and gas tanks, wagons and for automotive purposes, as well as different types of ships and ship parts (Chen et al., 2009; Engler and Hirsch, 2002; Johnson and Threadgill, 2003; Mendes et al., 2016). The FSW process results in high quality welds, with virtually no solidification cracking, porosity, oxidation

and other defects commonly found in fusion welding processes (Chao et al., 2003; Chen et al., 2009). Due to its energy efficiency, environment friendliness and versatility, the FSW process is considered a “green” and efficient technology. The FSW process therefore uses a non-consumable tool; no cover gas or flux is used, thus making the process environmentally friendly (Mishra and Ma, 2005; Thomas, 1998).

Friction stir welds of polymers, mild steel, non-ferrous metallic alloys, similar or dissimilar, in particular aluminium alloys, provide opportunities for the improvement and development of new product designs. In this type of welding, residual stresses, field distribution and crack propagation require a carefully thought-out tool design (Fratini and Pasta, 2012; Kallee et al., 2001), particularly in case of complex joints such as lap, overlap welds, T-sections and corner welds and welding positions like overhead and orbital, which are included in the project (ISO 25239-2:2011, 2011; Kallee et al., 2001; Thomas, 1998).

Aluminium alloys are suitable for friction stir welding process due to their relatively low solid-state welding temperature – approximately 80 % of Al melting point (660°C) (Callister, 2013; Hatch, 1984; Mishra, Partha and Kumar, 2014). Al alloys are likewise suitable for FSW processes due to their corrosion resistance (due to the formation of an adherent thin film of Al₂O₃) and low mass density (Al-Jarrah et al., 2014, Callister, 2013; Mishra, Partha and Kumar, 2014; Vargel, 2004).

The purpose of this paper is to analyse the mechanical behaviour and the microstructure of Al-Mg-Si-Cu alloy plates which are friction stir welded and heat treated in two different temper conditions.

2. TECHNICAL APPROACH

2.1. Aluminium Alloys in Shipbuilding

Recommendations for aluminium alloys used in shipbuilding, specific for hull construction and marine structures, are divided into two general groups – rolled and extruded products. Rolled plates, sheets and strips are manufactured using Al 5xxx series - AA 5083, 5086, 5383, 5059, 5754, 5454, 5456, 5474 aluminium alloys - usually alloyed with Mg under O, H112, H116 and H321 temper conditions. Extruded products – bars, profiles and shapes – are made from aluminium alloys AA 5083, 5383, 5059 and 5086 under O, H111, H112 temper conditions. Likewise, in the Al 6xxx series - AA 6005A, 6060, 6106, 6061, 6063, 6082 – Mg and Si are the dominant alloying elements used in T5 and T6 temper conditions (ASM Handbook vol 2 and 4, 2001; IACS, 2009; Hatch, 1984; Sielski 2007; SSC-452, 2007; Vargel, 2004).

Broad aluminium panels manufactured with the FSW process, used in cruise ships, catamarans and other high-speed ferries are the examples of typical applications (Kallee, 2000; Kallee, Nicholas and Thomas, 2001), as are the FSW of extruded Al

panels used for freezing fish onboard fishing ships, and extruded Al honeycomb and seawater resistant panels for hulls and decks, welded using the same process (Johnson and Threadgill, 2003; Kallee, 2000; Kallee, Nicholas and Thomas, 2001).

AA5xxx and AA6xxx plates and extrusions, and the FSW process are among the most common marine applications (Johnson and Threadgill, 2003). AA 6061, 6082 T6, AA 5083 and H112 and H116 were among the first aluminium alloy FSW joints to be commercially introduced into shipbuilding (Colligan, 2004; Johnson and Threadgill, 2003; Kallee, 2000; Kallee, Nicholas and Thomas, 2001).

The mechanical properties of 5xxx series aluminium alloys are usually improved by cold working. On the other hand, mechanical properties of 6xxx series alloys are improved considerably by the precipitation of coherent second phase particles after thermal treatment (Hatch, 1984).

Aluminium alloys with Cu additions, more specifically the AA6xxx and 7xxx-series Al, are used as medium-strength structural alloys, due to their good corrosion resistance and mechanical properties owing to the formation of fine intermetallic particles (Esmaily et al., 2016; Mishra, Partha and Kumar, 2014; Olea et al., 2007). AA5xxx-series aluminium alloys H116 under tempered condition have shown good corrosion resistance, especially to exfoliation corrosion (Mishra, Partha and Kumar, 2014; Vargel, 2004).

2.2. Friction Stir Welding Process

Developed by The Welding Institute (TWI), UK, in the early 1990's, the FSW process works by plunging a rotating tool into the joint until the tool's shoulder touches the joint line; then traversing the rotating tool along the joint, as shown schematically in Figure 1 (Mendes et al., 2016; Mishra and Ma, 2005; Thomas, 1991). The rotating tool is usually slightly tilted during the FSW process, within a tilt angle of maximum 3°, to ensure the necessary amount of torque and forces needed to obtain defect-free welds in the initial stages of welding (Banik et al., 2018).

The large plastic deformation around the rotating tool during the welding process and the friction between the tool and the workpieces are the two main heat generators in FSW. Both aspects increase temperature in and around the stirred zone, although friction is considered the major source of heat (Mishra and Ma, 2005; Olea, 2008; Mishra, Partha and Kumar, 2014).

The microstructural changes and the consequential altered mechanical operation of friction stir welded joints are important issues to be studied. The influence of the heat flow, rotation and welding speed on workpiece structure, mainly in the nugget and thermomechanical affected zone, are evident (Moreira et al., 2009; Mishra, Partha and Kumar, 2014). Dynamic recrystallization is likely to occur due to the temperature and pressure applied

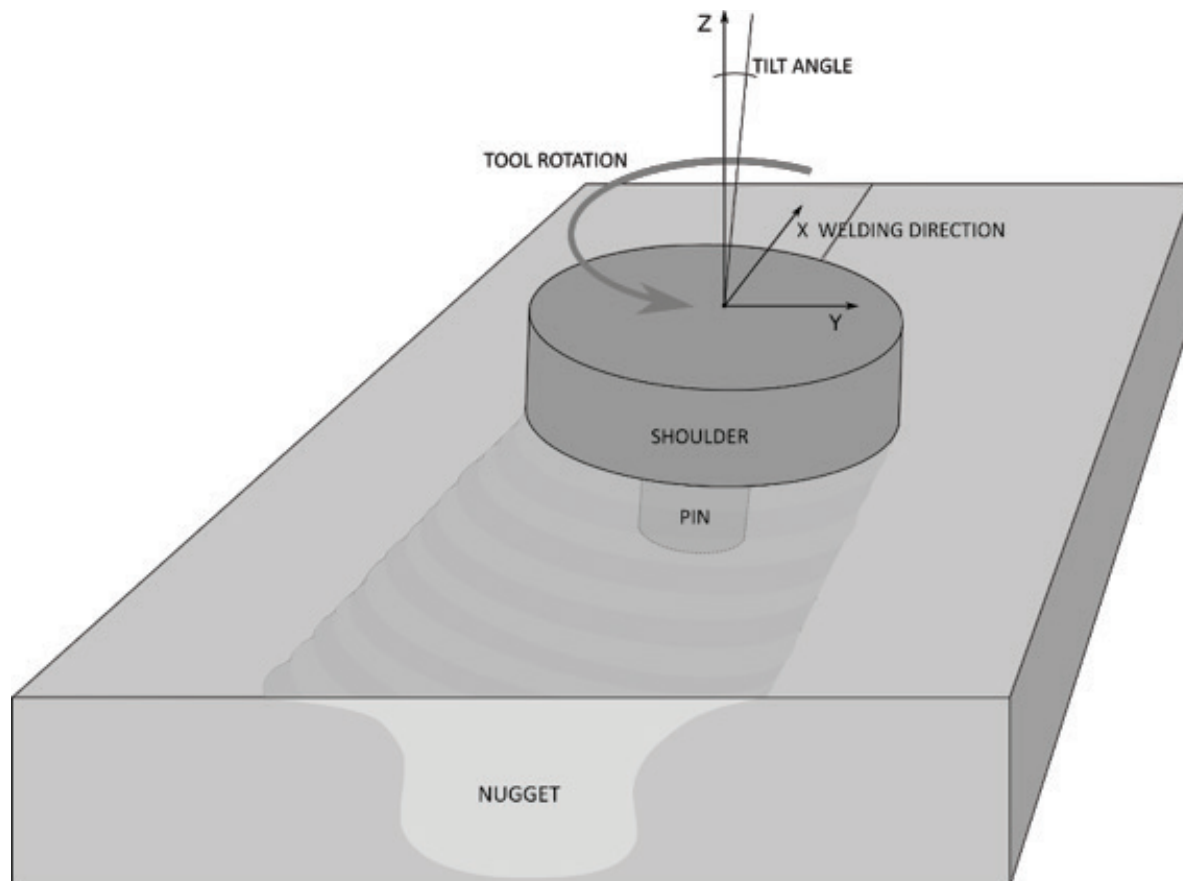


Figure 1.
Illustration of the FSW process.

during the FSW of aluminium alloys (Heinz and Skrotzki, 2002). The FSW process also causes a decrease in dislocation density and in the dissolution of the strengthening precipitates (Mishra and Ma, 2005; Sidhar et al., 2016). However, the mechanical properties of a post-weld heat treatment of heat-treatable aluminium alloys change significantly due to the formation of alloying element second phase particles, such as $\text{CuAl}_2 - \theta$ phase, $\text{Mg}_2\text{Si} - \beta$ phase and Q phase, a quaternary compound of Al-Cu-Mg and Si with varying stoichiometry and different morphologies (Chakrabarti, D. J. and Laughlin, 2004; Heinz and Skrotzki, 2002; Murayama et al., 2001; Olea et al., 2007, Sidhar et al., 2016; Vivas et al., 1997). According to Hill (2015) and Liu et al. (2018), when alloying elements such as Fe and Mn are kept at high temperatures, they might generate second phase particles which increase their volume fraction and particle size.

The FSW technology was developed using sophisticated robotic systems and software, facilitating the use of the FSW process in a wide range of industrial applications and working conditions (Mendes et al., 2016). Both experimental and

numerical analysis are important for understanding the heat flow and the transfer between the steel tool and the workpiece during the FSW process, and the weld morphology (Chao et al., 2003; Fratini et al., 2006; Sadeghian, Taherizadeh and Atapour, 2018; Zhao et al., 2018). Authors Ku, Ha and Roh (2014) developed a mobile welding robot and software controls to be used for welding double hull structures in shipyards. On the other hand, Cavaliere (2013), using a database obtained from experimental data, developed a friction stir weld mechanical behaviour prediction model. The model takes mechanical properties into consideration.

3. EXPERIMENT

Al-Mg-Si with Cu alloy 4 mm thick rolled plates were friction stir butt welded using a Tricept 805 robot with a CNC controller. The FSW was performed at rotational speed of 1600 rpm and tool transverse speed of 800 mm/min, with a 3° tilt. The investigated heat treatment conditions are listed in Table 1.

Table 1.

Description of the plate heat treatment.

Temper condition	Description
PWHT	FSW in T4 and heat treatment in an air furnace to T6 at 190°C for 4h (ASM Handbook vol. 4, 2001)
FSW T6	Artificially aged at 190°C for 4h and friction stir welded

Vickers microhardness profiles were obtained from the perpendicular cross section welding direction, using a HMV200 Shimadzu from Struers, with a Vickers indenter having the load of 100 gf (HV0.1). A 0.5 mm step between indentations was used along the centerline of the plates.

The tensile tests were performed using a servo-hydraulic INSTRON model 1195. In the conventional tensile test, full-scale load was 50 kN, with a test speed of 1 mm/min.

Optical microscopy (OM) samples were etched with Flick reagent (i.e. 10 ml HF, 15ml HCl and 90 ml deionized water) and analysed with an Olympus PMG3.

The morphologies of the grains and second phase particles were obtained by SEM, using a Zeiss DSM 962 device in SE and BSE modes. The chemical composition of the particles was obtained by energy dispersive X-Ray spectroscopy (EDS) with a Si-Li detector coupled with SEM.

Specimens were not etched in SEM analysis. The macro- and microstructures of the weld were revealed with Flick reagent (i.e. 10 ml HF, 15ml HCl and 90 ml deionized water) and analysed with an Olympus PMG3 optical microscope (OP).

The chemical composition of the base material in weight % is given in Table 2.

Table 2.

Composition of the Al-Mg-Si-Cu alloy (wt. %).

Elements	Mg	Si	Cu	Mn	Fe	Zn	Ti	Zr	Pb	Al
Wt. %	0.76	0.92	0.77	0.56	0.24	0.19	0.012	0.11	0.003	bal.

4. RESULTS AND DISCUSSION

The Al-6xxx series alloyed mainly with Mg, Si and Cu, also contains a fair amount of Mn and Fe. The alloying elements mostly contribute by increasing material hardness and strength by forming complex, intermetallic second phase particles and the substitutional solid solution (Hatch, 1984).

4.1. Mechanical testing

The relationship between macrostructure and microhardness, taken as a function of position along the weld cross section, is shown in Figure 1. The macrostructure presented in Figure 1(a) outlines the base material (BM) and the weld zones – heat-affected zone (HAZ), thermo-mechanically affected zone (TMAZ) and nugget zone (NZ). Figure 1(b) illustrates the Vickers

microhardness profile of Al-Mg-Si-Cu plates in FSW T4, FSW T4 + PWHT and FSW T6 conditions, measured along the centerline of the cross section.

The macrostructure of the weld is a source of information on the retreating and advancing sides, and facilitates clear identification of the NZ (coloured with a darker tone after etching). Also, the U-shape of the weld zone broadens at the top due to the firm contact between the shoulder of the tool and the upper surface – Figure 1(a).

The hardness profile of the plates showed that the hardness of the PWHT increased compared to the FSW T6, especially the TMAZ and NZ zones. Taking into consideration the lowest TMAZ and the highest NZ hardness values, the hardness of PWHT plates increased by approx. 20 HV in TMAZ and 40 HV in NZ when compared to FSW T6 hardness results – Figure 1(b). HAZ is not significantly affected by the FSW process.

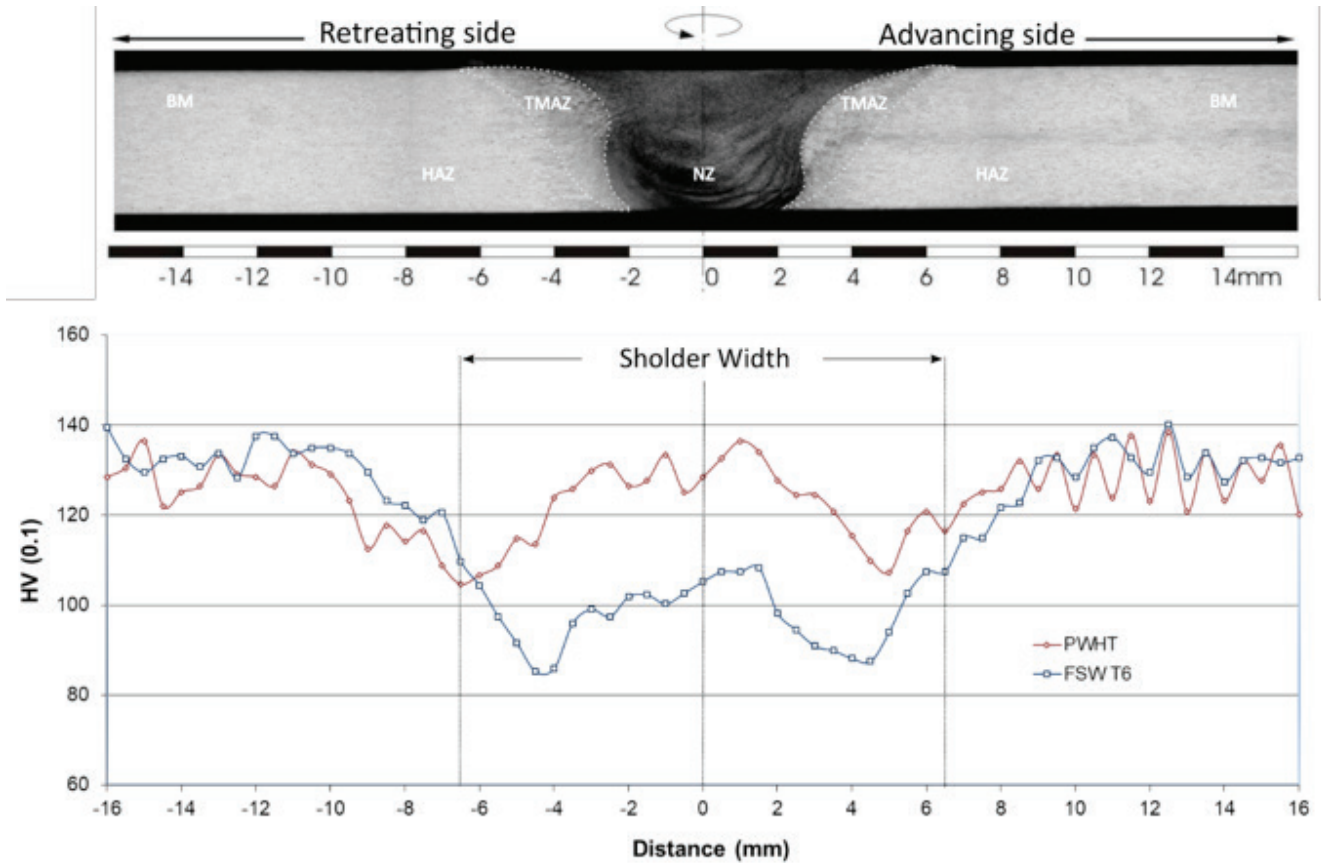


Figure 2.

(a) Macrostructure of the weld cross section and (b) Microhardness profiles of FSW PWHT and FSW T6.

Uniaxial tensile tests were performed at room temperature. The results for both base materials (BM) with welded components are given for an average of three specimens. Table 3 illustrates

the mechanical properties of the base material and welded specimens under T6 temper conditions.

Table 3.

Results of uniaxial tensile tests for the base material and welded specimens under given temper conditions.

Material:	$R_{p0.2}$	R_m	A[%]	WF		WF	
				R_p	$R_{0.2}$	R_m	A[%]
Al-Mg-Si-Cu	[MPa]	[MPa]		[%]		[%]	
BMT6	339	353	7	--	--	--	--
PWHT	318	329	1	94		93	14,3
FSW T6	218	299	4	64		85	57

$R_{p0.2}$ – yield strength; R_m – tensile strength; A – elongation.

WF – weld/joint efficiency (i.e. WF ratio between the static properties of the weld and of the BM).

A failure pattern was observed in TMAZ in the retreating side of the welds - Figure 2(a). Except in the welded tested specimens in T6 temper conditions, the value of WF exceeded 85 % for $R_{p0.2}$ and R_m , confirming the high strength of joints made by friction stir welds.

The yield strength ($R_{p0.2}$) and tensile strength (R_m) of PWHT tested specimens are in the range of the mechanical properties required for hull construction and marine structures. The results of the SSC-452 (2007) guide have shown that an AA 6082 T6 base material yielded 286 MPa and 301 MPa of $R_{p0.2}$ and R_m , respectively. The same AA 6082 Al alloy, friction stir welded in T6, delivered the yield strength of 160 MPa and tensile strength of 254 MPa. The PWHT results for the same alloy delivered 285 MPa and 310 MPa of $R_{p0.2}$ and R_m , respectively. The elongation % of the AA 6082 T6 base material and the T4 FSW, aged to T6, were approx. 10 % and 9 %, respectively (SSC-452, 2007).

5-50 mm thick sheets and plates for marine applications, made from 5xxx series aluminium alloys yielded $R_{p0.2}$ between 195 and 270 MPa and R_m between 250 and 438 MPa (Sielski, 2007).

The extruded products of Al 6xxx series alloys having the thickness of 3 and 50 mm require 170-200 MPa and 260 MPa of yield strength and 260 and 310 MPa of tensile strength in T6 temper conditions (IACS, 2009; Sielski 2007; SSC-452, 2007).

4.2. Morfology

Figure 4 shows the microstructure of the Al-6xxx alloy PWHT and FSW of the friction stir welded specimens from the SEM perspective. SEM image - Figure 4(a) shows the details of the interface between TMAZ and NZ, while Figure 4(b) shows NZ with small equiaxed recrystallized grains.

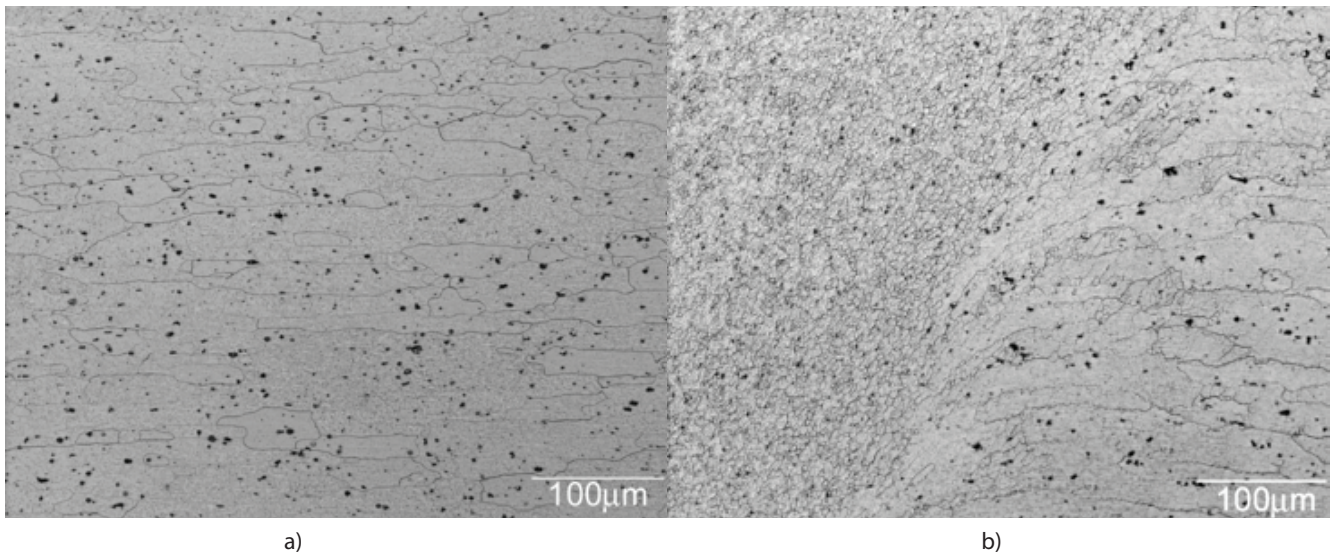


Figure 3.

OP images of the (a) base material grain morphology, and (b) interface between the nugget zone and the thermomechanically affected zone. Flick reagent.

Grain size and the morphology of friction stir welded plates in NZ, TMAZ and HAZ of PWHT and FSW T6 did not show significant changes.

The grain morphology along the weld zones of the Al-Mg-Si-Cu alloy PWHT changes under FSW T6 conditions - Figure 2(a). The BM represents elongated, pancake-shaped, 100-300 µm long grains on the BM - Figure 3(a) equiaxed 5.6 - 2.8 µm grains at NZ - Figures 3(b) and 4(b). Between the TMAZ and the NZ, there is a distinct interface of elongated grains twisted at 90° and small equiaxed grains - Figures 2(a), 3(b) and 4(a).

Figure 5 shows evenly distributed second phase particles - white spherical, oval and rod-shaped, having the average size between 100 and 500 nm - and coarse irregular micrometric particles. The SEM/EDS particle analysis from Figure 5 indicates the presence of Al-Cu-Mg-Si-Mn and Fe, suggesting the formation of Mg-Si, Al-Cu, Al-Cu-Mg-Si, and Al(Mn,Fe)Si second phase particles (Chakrabarti, D. J. and Laughlin, 2004; Hill, 2015). Previous work on Al-Mg-Si-Cu alloys using transmission electron microscopy (TEM) and the selected area diffraction pattern (SADP) indicate that the greatest contribution to alloy hardening

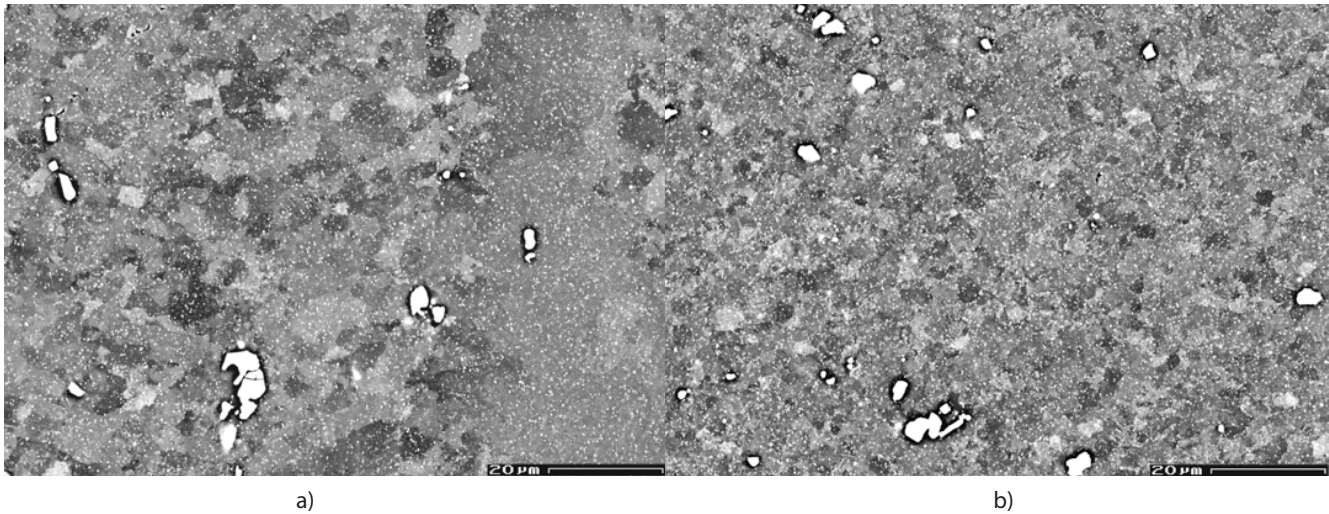


Figure 4.

SEM images of the weld (a) interface between NZ (small recrystallized grains) and TMAZ (elongated grain), and (b) nugget zone.

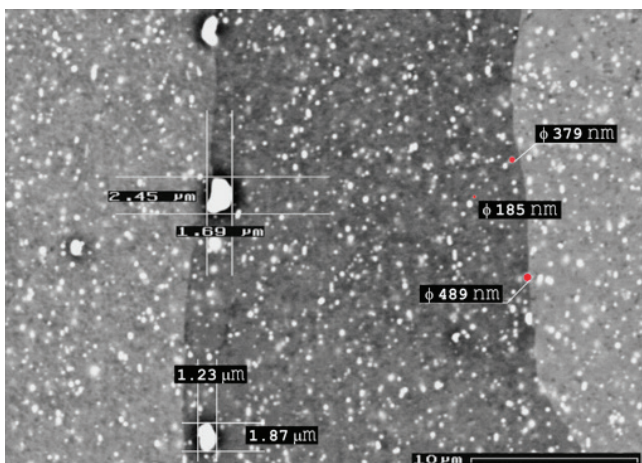


Figure 5.

SEM image - TMAZ zone under PWHT temper condition, with the sizes of several second phase particles.

and strengthening occurs in the Q phase (Al-Cu-Mg-Si particles) (Chakrabarti, D. J. and Laughlin, 2004; Olea et al., 2007; Gallais, 2008).

The grain refinement in NZ under the FSW T6 condition does not have the main role in material strengthening. For example, the BM T6 condition yields the strength of 339 MPa, which is considerable higher than the FSW T6 yield strength of 218 MPa. Under this condition, the extra heat generated by the high temperature of the FSW process (approximately 80 % of melting point) dissolved the strengthening precipitates in the Al

matrix. In addition, the contribution of coarse particles to alloy strengthening is low (Hill, 2015; Mishra and Ma, 2005; Sidhar et al., 2016). On the other hand, the PWHT - FSW in T4 and the 4-hour heat treatment of T6 at 190°C, resulted in only a minor decrease in hardness in comparison with BM yield strength. In this case, the heat treatment after friction stir welding greatly contributes to the precipitation of the strengthening Q phase precipitates (Chakrabarti, D. J. and Laughlin, 2004; Heinz and Skrotzki, 2002; Murayama et al., 2001; Sidhar et al., 2016).

The results of the microhardness profile correlate very well with the tensile test results. Hardness in NZ and TMAZ increased with the PWHT. FSW T6 small grain size in NZ compared with BM did not effectively contribute to the increase in hardness.

5. CONCLUSIONS

The results indicate there is a correlation between the mechanical properties and the microstructural evolution associated with the FSW solid-state welding process using the Al-Mg-Si-Cu alloy under PWHT and FSW T6 temper conditions.

The FSW joint had four distinct zones - BM, HAZ, TMAZ and NZ. BM and HAZ did not show significant alterations either in grain morphology and size, nor in mechanical properties in either of these temper conditions. The BM elongated pancake-shaped 100-300 μm long grains and the NZ equiaxed and 5.6-2.8 μm recrystallized grains were found. SEM also identified and measured second phase particles sized 100 nm - several μm.

The evaluation of the microhardness profile and tensile tests indicated that the TMAZ and the NZ of a joint welded

under the PWHT condition increased the strength along the joint, giving better results than FSW T6. These results indicate that the PWHT propitiated the formation of a significant amount of strengthening precipitates in the NZ, which increased the strength of the material. However, the decrease in grain size did not translate into a significant increase in material strength.

ACKNOWLEDGEMENTS

This paper is in memoriam of Liane Roldo's mentor and advisor Prof. Telmo Roberto Strohaecker, who passed away on 6th October 2016.

The correspondent author gratefully acknowledges the fellowship grant from the Brazilian National Council for Scientific and Technological Development – CNPq. In addition, we wish to thank the following who contributed with equipment and base material to carry out this research: the Brazilian Laboratories of Design and Materials Selection and Physical Metallurgy of Federal University of Rio Grande do Sul, Porto Alegre, as well as the German Centre for Materials and Coastal Research Helmholtz-Zentrum, Geesthach.

References

- Al-Jarrah, J.A. et al., 2014. Welding equality and mechanical properties of aluminum alloys joints prepared by friction stir welding. *Materials & Design* (1980-2015), 56, pp.929–936. Available at: <https://dx.doi.org/10.1016/j.matdes.2013.12.003>.
- ASM Handbook Vol. 4, 2001. Heat Treating, Ohio, ASM International.
- ASM Handbook Vol. 2, 2001. Properties and Selections: nonferrous alloys and special-purpose materials, Ohio, ASM International.
- Banik, A. et al., 2018. An experimental investigation of torque and force generation for varying tool tilt angles and their effects on microstructure and mechanical properties: Friction stir welding of AA 6061-T6. *Journal of Manufacturing Processes*, 31, pp.395–404. Available at: <http://dx.doi.org/10.1016/j.jmappro.2017.11.030>.
- Callister, W. D. and Rethwisch D. G., 2013. *Materials Science and Engineering: An Introduction*, 9th Edition, New York, Wiley.
- Cavaliere, P., 2013. Friction Stir Welding of Al Alloys: Analysis of Processing Parameters Affecting Mechanical Behavior. *Procedia CIRP*, 11, pp.139–144. Available at: <https://dx.doi.org/10.1016/j.procir.2013.07.039>.
- Cerri, E. & Leo, P., 2013. Influence of high temperature thermal treatment on grain stability and mechanical properties of medium strength aluminium alloy friction stir welds. *Journal of Materials Processing Technology*, 213(1), pp.75–83. Available at: <https://dx.doi.org/10.1016/j.jmatprotec.2012.09.001>.
- Chakrabarti, D. & Laughlin, D.E., 2004. Phase relations and precipitation in Al–Mg–Si alloys with Cu additions. *Progress in Materials Science*, 49(3-4), pp.389–410. Available at: [https://dx.doi.org/10.1016/s0079-6425\(03\)00031-8](https://dx.doi.org/10.1016/s0079-6425(03)00031-8).
- Chao, Y.J., Qi, X. & Tang, W., 2003. Heat Transfer in Friction Stir Welding—Experimental and Numerical Studies. *Journal of Manufacturing Science and Engineering*, 125(1), pp.138–145. Available at: <https://dx.doi.org/10.1115/1.1537741>.
- Chen, Y.C., Feng, J.C. & Liu, H.J., 2009. Precipitate evolution in friction stir welding of 2219-T6 aluminum alloys. *Materials Characterization*, 60(6), pp.476–481. Available at: <https://dx.doi.org/10.1016/j.matchar.2008.12.002>.
- Colligan, K. J., 2004. Friction Stir Welding for Ship Construction: enables prefabricated, stiffened panels with low distortion, Navy Metalworking Center, Concurrent Technologies Corporation (CTC). Available at: <http://www.nmc.ctc.com/useruploads/file/publications/FSWShipConstruction.pdf>.
- Engler, O. & Hirsch, J., 2002. Texture control by thermomechanical processing of AA6xxx Al–Mg–Si sheet alloys for automotive applications—a review. *Materials Science and Engineering: A*, 336(1-2), pp.249–262. Available at: [http://dx.doi.org/10.1016/s0921-5093\(01\)01968-2](http://dx.doi.org/10.1016/s0921-5093(01)01968-2).
- Esmaily, M. et al., 2016. Bobbin and conventional friction stir welding of thick extruded AA6005-T6 profiles. *Materials & Design*, 108, pp.114–125. Available at: <http://dx.doi.org/10.1016/j.matdes.2016.06.089>.
- Fratin, L. et al., 2006. Material flow in FSW of AA7075–T6 butt joints: numerical simulations and experimental verifications. *Science and Technology of Welding and Joining*, 11(4), pp.412–421. Available at: <https://dx.doi.org/10.1179/174329306x113271>.
- Fratin, L. & Pasta, S., 2011. Residual stresses in friction stir welded parts of complex geometry. *The International Journal of Advanced Manufacturing Technology*, 59(5-8), pp.547–557. Available at: <https://dx.doi.org/10.1007/s00170-011-3510-4>.
- Gallais, C. et al., 2008. Precipitation microstructures in an AA6056 aluminium alloy after friction stir welding: Characterisation and modelling. *Materials Science and Engineering: A*, 496(1-2), pp.77–89. Available at: <https://dx.doi.org/10.1016/j.msea.2008.06.033>.
- Galvão, I. et al., 2010. Material flow in heterogeneous friction stir welding of aluminium and copper thin sheets. *Science and Technology of Welding and Joining*, 15(8), pp.654–660. Available at: <https://dx.doi.org/10.1179/136217110x12785889550109>.
- Hatch J. E., 1984. *Aluminium Properties and Physical Metallurgy*. Ohio, Aluminum Association Inc. and ASM International.
- Heinz, B. & Skrotzki, B., 2002. Characterization of a friction-stir-welded aluminum alloy 6013. *Metallurgical and Materials Transactions B*, 33(3), pp.489–498. Available at: <http://dx.doi.org/10.1007/s11663-002-0059-5>.
- Hill, T. C., 2015. Evolution of second phase particles with deformation in aluminium alloys, Thesis, School of Materials, University of Manchester. Available at: https://www.research.manchester.ac.uk/portal/files/61847259/FULL_TEXT.PDF.
- ISO 25239-2:2011, 2011. Friction Stir Welding — Aluminium, Part 2: Design of Weld Joints European Committee for Standardization.
- Johnson, R. and Threadgill, P. L., 2003. Progress in friction stir welding of aluminium and steel for marine applications, RINA Conference: Advanced Marine Materials: Technology and Applications, London, England, October 9 – 10. Available at: <https://www.twi-global.com/technical-knowledge/published-papers/progress-in-friction-stir-welding-of-aluminium-and-steel-for-marine-applications-october-2003/>
- Kallee, S. W., 2000. Application of friction stir welding in the shipbuilding industry, Lightweight Construction - Latest Developments, The Royal Institution of Naval Architects, London, England, February 24 – 25. Available at: <https://www.twi-global.com/technical-knowledge/published-papers/application-of-friction-stir-welding-in-the-shipbuilding-industry-february-2000/>

- Kallee, S.W., Nicholas, E. D. and Thomas, W. M., 2001. Friction stir welding - invention, innovations and application, INALCO, 8th Intl. Conf. on Joints in Aluminium, Munich, Germany, March 28 – 30. Available at: <https://www.twi-global.com/technical-knowledge/published-papers/friction-stir-welding-invention-innovations-and-applications-march-2001/>.
- Ku, N., Ha, S. & Roh, M.-I., 2014. Design of controller for mobile robot in welding process of shipbuilding engineering. *Journal of Computational Design and Engineering*, 1(4), pp.243–255. Available at: <http://dx.doi.org/10.7315/jcde.2014.024>.
- Leal, R.M. et al., 2008. Material flow in heterogeneous friction stir welding of thin aluminium sheets: Effect of shoulder geometry. *Materials Science and Engineering: A*, 498(1-2), pp.384–391. Available at: <http://dx.doi.org/10.1016/j.msea.2008.08.018>.
- Liu, C.L. et al., 2018. The interaction between Mn and Fe on the precipitation of Mn/Fe dispersoids in Al-Mg-Si-Mn-Fe alloys. *Scripta Materialia*, 152, pp.59–63. Available at: <http://dx.doi.org/10.1016/j.scriptamat.2018.04.012>.
- Malopheyev, S. et al., 2016. Optimization of processing-microstructure-properties relationship in friction-stir welded 6061-T6 aluminum alloy. *Materials Science and Engineering: A*, 662, pp.136–143. Available at: <http://dx.doi.org/10.1016/j.msea.2016.03.063>.
- Mendes, N. et al., 2016. Machines and control systems for friction stir welding: A review. *Materials & Design*, 90, pp.256–265. Available at: <http://dx.doi.org/10.1016/j.matdes.2015.10.124>. Mishra, R. S. and Ma, Z. Y., (2005), Friction stir welding and processing, *Materials Science and Engineering R* 50 (1-2), pp. 1–78, <http://dx.doi.org/10.1016/j.mser.2005.07.001>.
- Mishra R. S., Partha, S. D. and Kumar, N., 2014. Friction Stir Welding and Processing: science and engineering. Springer International Publishing, Switzerland. Available at: <https://link.springer.com/content/pdf/10.1007/978-3-319-07043-8.pdf>.
- Moreira, P.M.G.P. et al., 2009. Mechanical and metallurgical characterization of friction stir welding joints of AA6061-T6 with AA6082-T6. *Materials & Design*, 30(1), pp.180–187. Available at: <https://dx.doi.org/10.1016/j.matdes.2008.04.042>.
- Murayama, M. et al., 2001. The effect of Cu additions on the precipitation kinetics in an Al-Mg-Si alloy with excess Si. *Metallurgical and Materials Transactions A*, 32(2), pp.239–246. Available at: <https://dx.doi.org/10.1007/s11661-001-0254-z>.
- Olea, C.A.W. et al., 2007. A sub-structural analysis of friction stir welded joints in an AA6056 Al-alloy in T4 and T6 temper conditions. *Materials Science and Engineering: A*, 454-455, pp.52–62. Available at: <https://dx.doi.org/10.1016/j.msea.2006.12.055>.
- Olea, C. A. W., 2008. Influence of Energy Input in Friction Stir Welding on Structure Evolution and Mechanical Behaviour of Precipitation-Hardening in Aluminium Alloys (AA2024-T351, AA6013-T6 and Al-Mg-Sc), Dissertation, ISSN 0344-9629, GKSS-Forschungszentrum – Helmholtz Gemeinschaft, Geesthacht, Germany. Available at: https://www.hzg.de/imperia/md/content/hzg/zentrale_einrichtungen/bibliothek/berichte/gkss_berichte_2008/gkss_2008_8.pdf.
- IACS - International Association of Classification Societies, 2009. Requirements Concerning Materials and Welding - W25, pp. 1 - 11.
- Robson, J.D., Upadhyay, P. & Reynolds, A.P., 2010. Modelling microstructural evolution during multiple pass friction stir welding. *Science and Technology of Welding and Joining*, 15(7), pp.613–618. Available at: <https://dx.doi.org/10.1179/136217110x12813393169651>.
- Sadeghian, B., Taherizadeh, A. & Atapour, M., 2018. Simulation of weld morphology during friction stir welding of aluminum- stainless steel joint. *Journal of Materials Processing Technology*, 259, pp.96–108. Available at: <http://dx.doi.org/10.1016/j.jmatprotec.2018.04.012>.
- Sidhar, H. et al., 2016. Friction stir welding of Al-Mg-Li 1424 alloy. *Materials & Design*, 106, pp.146–152. Available at: <https://dx.doi.org/10.1016/j.matdes.2016.05.111>.
- Sielski, R. A., 2007. Review of Structural Design of Aluminum Ships and Craft, *Transactions TRANS*, pp. 1-30. Available at: https://www.researchgate.net/publication/290899673_Review_of_structural_design_of_aluminum_ships_and_craft.
- SSC-452, *Aluminum Structure Design and Fabrication Guide*, 2007. Ship Structure Committee. Washington DC, 2-3. Available at: <https://www.shipstructure.org/pdf/452-II.pdf>, accessed on: March 27th 2018.
- Sun, Y.F. et al., 2013. Microstructure and mechanical properties of dissimilar Al alloy/steel joints prepared by a flat spot friction stir welding technique. *Materials & Design*, 47, pp.350–357. Available at: <https://dx.doi.org/10.1016/j.matdes.2012.12.007>.
- Thomas, W., 1991. Friction Stir welding, The Welding Institute – TWI Ltd. Available at: <https://www.twi-global.com/capabilities/joining-technologies/friction-welding/friction-stir-welding/>.
- Thomas, W., 1998. Friction stir welding and related friction process characteristics, INALCO '98, 7th International Conference on Joints in Aluminium, Cambridge, United Kingdom, April 15 – 17. Available at: <https://www.twi-global.com/technical-knowledge/published-papers/friction-stir-welding-and-related-friction-process-characteristics-april-1998/>.
- Vargel, C., 2004. Aluminium and the Sea, Alcan Marine, pp. 33 – 199. Available at: <http://www.ansatt.hig.no/henningj/materialteknologi/lvd-aluminium%20and%20the%20sea.htm>.
- Velichko, O.V. et al., 2016. Structure and Properties of Thick-Walled Joints of Alloy 1570s Prepared by Friction Stir Welding. *Metal Science and Heat Treatment*, 58(5-6), pp.346–351. Available at: <http://dx.doi.org/10.1007/s11041-016-0015-7>.
- Vivas, M. et al., 1997. Transmission electron microscopy study of precipitate morphology and precipitate overcoming processes in aluminum alloy 6056 T6. *Materials Science and Engineering: A*, 234-236, pp.664–667. Available at: [http://dx.doi.org/10.1016/s0921-5093\(97\)00274-8](http://dx.doi.org/10.1016/s0921-5093(97)00274-8).
- ZHAO, P. et al., 2018. Numerical simulation of friction stir butt-welding of 6061 aluminum alloy. *Transactions of Nonferrous Metals Society of China*, 28(6), pp.1216–1225. Available at: [http://dx.doi.org/10.1016/s1003-6326\(18\)64759-4](http://dx.doi.org/10.1016/s1003-6326(18)64759-4).